

# Investigation of precipitate hardening of slip and twinning in Mg5%Zn by micropillar compression



Jiangting Wang, Nicole Stanford

Institute for Frontier Materials, Deakin University, Geelong, VIC 3217, Australia

## ARTICLE INFO

### Article history:

Received 15 May 2015

Revised 28 July 2015

Accepted 7 August 2015

### Keywords:

Micropillar compression

Magnesium alloy

Precipitates

Twinning

Slip

## ABSTRACT

A Mg-5%Zn alloy has been aged to form *c*-axis rod precipitates which are known to increase strength. Micropillar compression tests were carried out in the precipitate-free and aged samples to investigate the effects of these precipitates on twinning and slip in magnesium alloys. Basal slip, pyramidal slip and  $\{10\bar{1}2\}$  twinning were selectively activated by compressing micropillars in the  $[11\bar{2}3]$ ,  $[0001]$  and  $[11\bar{2}0]$  orientations, respectively. It has been found that precipitation causes moderate hardening of the basal slip system, and also significantly increases the work hardening rate. The compression of  $[11\bar{2}0]$  initiated twinning, but the present experiments were dominated by twin nucleation, rather than growth. It was found that the effect of precipitation on twin nucleation was negligible. Precipitation had little effect on specimens compressed in the *c*-axis.

Crown Copyright © 2015 Published by Elsevier Ltd. on behalf of Acta Materialia Inc. All rights reserved.

## 1. Introduction

High specific-strength magnesium alloys have potential applications in the automotive and aircraft industries due to the high demand for weight reduction and fuel efficiency [1]. Precipitation hardening is a promising way to strengthen magnesium alloys [2–9] and reduce their mechanical asymmetry [10,11]. Unlike the more common metallurgical systems, magnesium has an HCP crystal structure which provides four principle deformation modes: slip on the basal plane, slip on the prismatic plane, slip on the pyramidal plane, and twinning on the  $\{10\bar{1}2\}$  plane [1,12]. At larger strains an additional twinning mode can also be activated on the  $\{10\bar{1}1\}$  plane. Due to the complexity of the deformation of this alloy system, standard test methods such as the Vickers hardness test do not provide any insight into the relative strengthening of the individual deformation modes, rather, these test methods simply inform us that macroscopically, the material is harder. Without an in-depth understanding of the ways in which precipitates strengthen the individual deformation modes, we are unable to design microstructures and precipitate populations for maximum strengthening benefit.

In particular, the interaction between precipitates and twinning remains unclear. There is general consensus in the literature that precipitation will increase the yield stress for polycrystals oriented for profuse twinning [6,13,14], but some authors report

this to be commensurate with a decrease in the twin volume fraction [4,10], while others show the volume fraction to be unaffected by precipitation [13]. The effect of precipitate morphology on the hardening of slip and twinning has been treated theoretically [15,16], but the outcome of these predictions are yet to be verified experimentally. The underpinning problem in measuring the precipitate strengthening of an individual deformation mode is that in polycrystalline materials it is not possible to activate only one mode. Utilising highly textured materials to make one deformation mode more dominant than others has been utilised successfully [6], but separation of the contributions of basal slip and twinning to the compressive flow stress remains a hindrance to conclusively quantifying the relative hardening increments of these modes. There is also some suggestion in the literature that the relative size of the precipitate and the twin may modify the twin morphology [17], and presumably, twin volume fraction. At present, the only dedicated study that has successfully examined the effect of precipitation on the individual deformation modes has been an in situ neutron diffraction study by Agnew et al. [18]. That study confirmed that precipitation hardened the basal slip system, but indicated that precipitation did not necessarily increase the stress to initiate twinning. This is in contradiction with most published literature on the topic. The source of these inconsistencies is likely to lie in the extremely high sensitivity of magnesium deformation to grain size, the fact that in some cases magnesium can form extremely strong textures, and the fact that we are not certain at present how solutes may be affecting these experiments.

E-mail addresses: [jiangting.wang@deakin.edu.au](mailto:jiangting.wang@deakin.edu.au) (J. Wang), [nicole.stanford@deakin.edu.au](mailto:nicole.stanford@deakin.edu.au) (N. Stanford)

Clearly, there is a strong need to approach this problem with a new experimental methodology. Since polycrystalline deformation concurrently activates multiple deformation modes, in this work, we designed a micropillar compression test to activate only one deformation mode. These experiments are essentially single crystal tests, and were designed to develop a more fundamental understanding of the effect of precipitation on slip and on deformation twinning. Several similar studies have been carried out in the past [19–27], but the effect of precipitation is yet to be explored in this way.

## 2. Experimental methods

As-extruded and aged Mg5%Zn samples from a previous study [6] were mechanically polished and finished with 0.05  $\mu\text{m}$  colloidal silica. Then, the specimens were lightly etched in Nital (5% nitric acid in ethanol) for approximately 2 s to remove any residual colloidal silica from the surface and reveal the grain boundaries. Crystal orientations were identified by electron backscatter diffraction (EBSD) technique using a FEG-SEM (FEI Quanta 3D) equipped with an EDAX-EBSD system. These EBSD maps were used to identify the grain orientations of interest. Micropillars oriented in  $[1\bar{1}20]$ ,  $[1\bar{1}23]$ , and  $[0001]$  directions were fabricated by focused ion beam (FIB) milling, with a Ga<sup>+</sup> ion beam operated at 30 kV. The beam current was 5 nA for coarse milling and then reduced to 50 pA for final polishing to minimise the ion beam damage. The FIB-prepared micropillars were  $\sim 2\ \mu\text{m}$  in diameter and  $\sim 4\ \mu\text{m}$  in height, with a taper angle of 2–3°. A typical example is shown in Fig. 1a.

Compression tests were carried out using a diamond flat punch (5  $\mu\text{m}$  in diameter) in a nanoindentation apparatus (UMIS, CSIRO). A schematic is shown in Fig. 1b. The flat punch was driven in a force-controlled mode to compress the micropillar with an estimated displacement rate of  $\sim 2.0\ \text{nm/s}$ , which corresponds to an approximate strain rate of  $5 \times 10^{-4}\ \text{s}^{-1}$ . The stress–strain curves were determined from the load–displacement curves and initial geometries of the micropillars [28,29]. The total displacement of the flat punch consists of two components, the length change of the pillar  $\Delta l$  and the displacement caused by the Sneddon's effects,  $u_{\text{Sneddon}}$ , which accounts for the elastic penetration of the pillar into the substrate. It can be written as

$$u_{\text{total}} = \Delta l + u_{\text{Sneddon}} \quad (1)$$

The displacement that the pillar penetrates into the substrate can be approximated using the Sneddon's solution for an isotropic elastic half space indented by a rigid circular flat punch [30],

$$u_{\text{Sneddon}} = \frac{(1 - \nu^2)P}{2E} \sqrt{\frac{\pi}{A_s}} \quad (2)$$

in which,  $E$  and  $\nu$  are the Young's modulus and Poisson's ratio, respectively.  $P$  is the loading force and  $A_s$  is the cross-sectional area of pillar base. By substituting Eq. (2) into (1), the length change  $\Delta l$  can be calculated as,

$$\Delta l = u_{\text{total}} - \frac{(1 - \nu^2)P}{2E} \sqrt{\frac{\pi}{A_s}} \quad (3)$$

Thus, the engineering strain  $\varepsilon_E$  and stress  $\sigma_E$  can be calculated as

$$\varepsilon_E = \frac{\Delta l}{l_0} \quad (4)$$

$$\sigma_E = \frac{P}{A_0} \quad (5)$$

where,  $l_0$  and  $A_0$  are the initial length and cross-sectional area of the pillar, respectively. The loading force  $P$  and total displacement  $u_{\text{total}}$

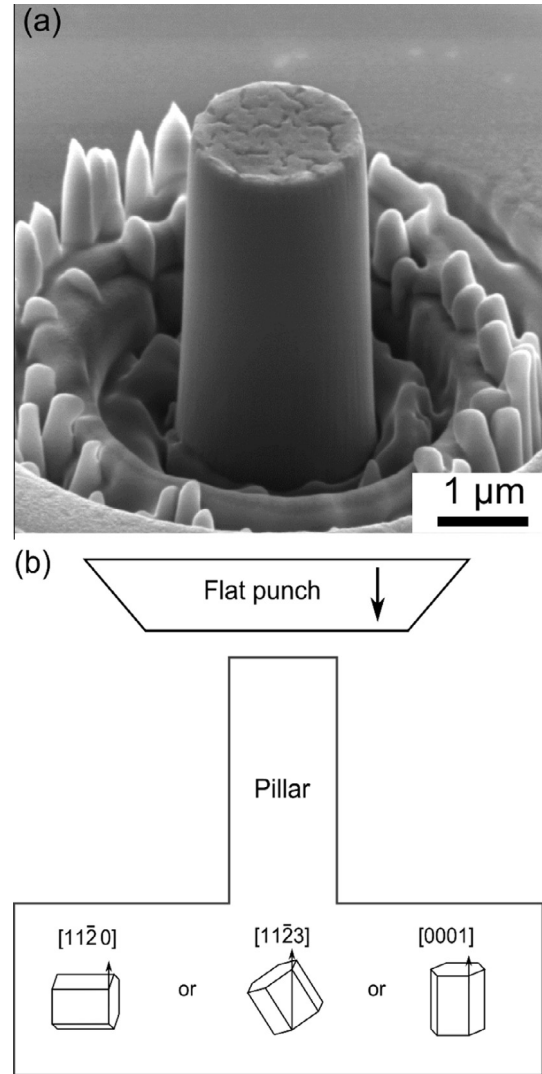


Fig. 1. (a) A typical micropillar of Mg5%Zn prepared by FIB milling. (b) Schematic of micropillar compression along particular crystal orientations.

are directly extracted from compression tests. The initial length and cross-sectional area of the micropillars are measured from SEM images. After compression, the deformed micropillars were cross-sectioned and lift-out for transmission electron microscopy (TEM) and transmission EBSD (t-EBSD). The specimens were thinned to  $\sim 200\ \text{nm}$  thick and finally polished with ion beam operated at 2 kV. T-EBSD mapping was carried out in FEG-SEM (FEI Quanta 3D) with the specimen oriented horizontally. The electron beam was operated at 30 kV with a beam current of 8 nA. The t-EBSD maps were collected at step size of 10 nm. The TEM studies were carried out using a JOEL 2100F operated at 200 kV.

## 3. Results

### 3.1. Precipitate distribution in aged Mg5%Zn

The as-extruded magnesium alloy is precipitate-free [6]. The precipitation treatment chosen for study in the present case was 150  $^{\circ}\text{C}$  for 8 days [6]. The precipitates formed by this treatment are shown in Fig. 2. The MgZn' precipitates are rod-shaped (as previously described in Refs. [3,6,8,9]), with the long axis of the rods being parallel to the  $c$ -axis of the matrix, i.e. parallel to the  $[0001]$  direction of the matrix. The length of the rods ranged from

Download English Version:

<https://daneshyari.com/en/article/7879311>

Download Persian Version:

<https://daneshyari.com/article/7879311>

[Daneshyari.com](https://daneshyari.com)